Structures of Hydrated Li^+−Thymine and Li^+−Uracil Complexes by IRMPD Spectroscopy in the N−H/O−H Stretching Region

Elizabeth A. L. Gillis, Khadijeh Rajabi, and Travis D. Fridgen*

Department of Chemistry, Memorial University of Newfoundland, St. John's, Newfoundland and Labrador, Canada A1B 3X7

Received: November 12, 2008; Revised Manuscript Received: November 25, 2008

The interaction of lithium ions with two pyrimidine nucleobases, thymine and uracil, as well as the solvation of various complexes by one and two water molecules, has been studied in the gas phase. IRMPD spectra are reported for each of $B-Li^+-(H_2O)_n$ ($n = 1-2$) and $B_2-Li-(H_2O)_m$ ($m = 0-1$) for B = thymine, uracil over the 2500−4000 cm^{-1} region. Calculations were performed using the B3LYP density functional in conjunction with the 6-31+G(d,p) basis set to model the vibrational spectra as well as MP2/6-311++G(2d,p) theory to model the thermochemistry of potential structures. Experimental and theoretical results were used in combination to determine structures of each complex, which are reported here. The lithium cation in all complexes was found to bond to the O4 oxygen in both thymine and uracil, and the first two water molecules of solvation were found to bond to Li^+. The experimental spectra obtained for $BLi^+(H_2O)_n$ ($n = 1-2$) and B_2Li^+ for thymine and uracil clearly resemble one another, suggesting similar structural features in terms of bonding between the base and Li^+, as well as for solvation. This was confirmed through theoretical work. The addition of water to the lithium ion-bound DNA base dimers has been shown to induce a significant change in structure of the dimer to a hydrogen-bonded system similar to base pairing in the Watson−Crick model of DNA.

1. Introduction

The presence of metal ions in biological systems can have a significant effect on the processes occurring within that system. Specifically, the effect of metal binding to DNA can have considerable consequences depending on the location of binding.[1] A stabilizing effect is observed when the metal ion interacts with a phosphate group of the nucleic acid chain due to charge neutralization. However, bonding of nucleic acid bases with metal ions leads to competition for the hydrogen-bonding system of Watson−Crick pairs, bringing about a disruption in the double helix.[1−3] Williams and co-workers[4] have identified monovalent metal cations in the minor groove of DNA using X-ray diffraction and NMR spectroscopy. AT-tracts have been found to associate to significant amounts of monovalent cations. The 5′A_pT3′ steps are thought to bind hard monovalent cations with four oxygen atoms from DNA and two from water.[5] These solvated cations obviously affect the structure of DNA and therefore recognition processes. It is thus advantageous to investigate the interaction between nucleobases and metal ions to further understand the role of metal ions in DNA processes.

Uracil and thymine are two pyrimidine nucleobases that form base pairs with adenine in RNA and DNA, respectively.[6] The interaction of metal ions with these molecules has proven to be a popular avenue of study with previous works having reported their interaction with various metal cations including Na^+, Mg^{2+}, K^+, Ca^{2+}, Zn^{2+}, and Pb^{2+}.[2,7−16] Interactions with the lithium ion, which is of particular interest in this study, have also been previously examined by various techniques.[2,9,10,13−17] Metal ion binding energies are defined as the negative of the dissociation energy of the $B-M^m$ bond in the complex[11] according to the following reaction

$$B + M^m \rightarrow BM^m$$

where B is the base and M is the metal ion with charge *m*. The metal ion binding energies of various nucleobases in the gas phase, including thymine and uracil, have been reported.[11] In particular, the litium cation affinities have been presented.[10,15,18]

Tautomerism should be considered when looking at the structure of metal ions interacting with nucleobases (Scheme 1). Multiple studies have focused on the energetics of these structures in the case of uracil and thymine,[19−21] while others have further examined tautomers in terms of their interaction with metal cations such as Na^+, Mg^{2+}, and Zn^{2+} with thymine[8,16] as well as the protonated forms of uracil and thymine.[22] In fact, Russo et al.[15] determined computationally that the canonical forms of Li^+−uracil and Li^+−thymine where Li^+ is bound to O4 are the lowest in energy. While the canonical structure is the lowest energy structure, Kabelac et al.[8] and Monajjemi et al.[16] demonstrate that the interaction with metal cations can help stabilize higher energy tautomers to a point where they are lower than that of the canonical structure. For these reasons we explore the structures of Li^+ bound to different tautomers of uracil and thymine as well as their solvated analogues.

The interaction of a molecule with its environment can affect the chemical processes that molecule undergoes. To be able to understand and predict the interactions of these bases in their natural environment (aqueous), one must understand their interactions with water and the role it plays in hydrogen bonding.[23] Previous studies have examined the interaction of thymine and uracil with water, including reports of hydration shells and clustering.[23−36] Microhydration, or the addition of water one unit at a time to a molecule of interest, allows one to investigate how the properties of that molecule change during the solvation process.[29] In the present study, the structure of the ion−water complex such as the most favorable binding sites of water is of interest.

* Author to whom correspondence should be addressed. E-mail: tfridgen@mun.ca.

10.1021/jp809993k CCC: $40.75
Published on Web 12/24/2008

SCHEME 1

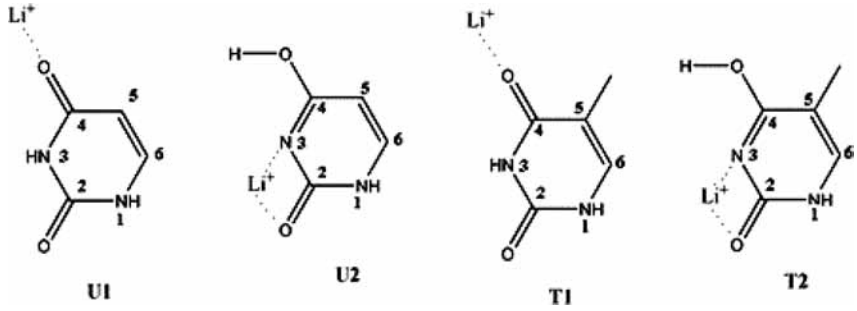

Experimental and theoretical infrared spectra of uracil and thymine in the gas and matrix isolation phases have been reported[37−42] as well as the IRMPD spectra of protonated uracil and thymine.[22] Infrared spectroscopy has proven to be a useful tool in examining structural characteristics of complexes involving nucleobases. For example, gas phase spectra of uracil and thymine clusters provided evidence of the presence of a variety of double hydrogen-bonded dimers.[23] In this study, we use IRMPD spectroscopy in combination with density functional theory calculations to determine the structure of lithium cationized uracil and thymine, including the litium ion-bound dimers of these nucleic acid bases, and the effect solvent has on their structures.

2. Methods

2.1. Experimental. The details of coupling the ApexQe Bruker Fourier transform ion cyclotron resonance (FT-ICR) mass spectrometer with a 25 Hz Nd:YAG pumped Laservision optical parametric oscillator/amplifier(OPO/OPA) laser have been presented previously.[43] Thymine, uracil, and lithium chloride used in this study were purchased from Sigma-Aldrich and were used without further purification. Solutions of 1 mM thymine, uracil, and LiCl were prepared in 18 MΩ Millipore water with LiCl added dropwise to 10 mL of the thymine/uracil solutions. Solvation was done in the accumulation/collision hexapole by replacing Ar trapping gas with water as described previously by Rajabi et al.[44] Ions were stored in the hexapole for 1−3 s in 10^{-2} torr water vapor to effect solvation after which they were transferred to the ICR cell and the ion of interest was isolated. Absorption of the infrared laser light caused dissociations of the complex under study. Scan rates ranged between 0.3 and 0.5 cm^{-1} s^{-1} and irradiation times between 0.15 and 2.0 s. This corresponds to a step size of between 1 and 4 cm^{-1} between points in the IRMPD spectra. IRMPD efficiency is defined as the negative of the natural logarithm of precursor ion intensity divided by the sum of the fragment and precursor ion intensities.

2.2. Computational. Calculations were performed using the Gaussian 03 suite of programs[45] with input created using Gaussview 3.0.[46] Geometry optimizations and frequency calculations of complexes were performed using the B3LYP density functional and 6-31+G(d,p) basis function. All calculated frequencies were scaled by a factor of 0.958 in accordance with that suggested for the level of theory and basis set.[47] The predicted spectra were convoluted with a Lorentzian profile with a fwhm of 2 cm^{-1}, significantly better resolution than the experimental spectra as evidenced by the figures. This resolution over a poorer resolution was chosen so all bands in the computed spectra could be seen in the figures. Additional single-point energy calculations were completed at the MP2 level of theory with the 6-311++G(2d,p) basis set on the B3LYP/6-31+G(d,p) geometries. The reported thermochemical results are a combination of the MP2/6-311++G(2d,p) electronic energies using unscaled thermal corrections and entropies from the B3LYP/6-31+G(d,p) calculations and are designated as MP2/6-311++G(2d,p)//B3LYP/6-31+G(d,p) thermochemistries.

3. Results and Discussion

The observed dissociation pathways of the solvated monomer, solvated dimer, and lithium-bound dimer were as expressed in eqs 1−3, respectively.

$$B_2Li^+ \rightarrow BLi^+ + B \quad (1)$$

$$BLi^+(H_2O)_n \rightarrow BLi^+(H_2O)_{n-1} + H_2O \quad (2)$$

$$B_2Li^+H_2O \rightarrow B_2Li^+ + H_2O \quad (3)$$

IRMPD spectra were collected for each of $B-Li^+-(H_2O)_n$ and $B_2-Li^+-(H_2O)_m$ (B = thymine, uracil, $n = 1$ or 2, and $m = 0$ or 1) and are compared in Figure 1. The spectra and structures of hydrated uracil−Li^+ and thymine−Li^+ (Ura-Li^+ and Thy-Li^+) will be discussed followed by the doubly hydrated species. The next species to be discussed will be the Li^+-bound dimers of uracil and thymine followed by the singly hydrated Li^+-bound dimer. The spectra of the nonsolvated B−Li^+ were not recorded since the expected IRMPD product, Li^+ at m/z 7 which was observed in collision-induced dissociation experiments,[10] is outside the mass range of the FTICR.

3.1. Ura-Li^+H_2O and Thy-Li^+H_2O. The IRMPD spectra recorded for Ura-Li^+ and Thy-Li^+ solvated by one water molecule are reported in Figures 2A and 2B, respectively. The ordinate on these IRMPD spectra is IRMPD efficiency. The very flat baseline is a result of no measureable product (no measureable IRMPD) being observed in the mass spectrum where there is no infrared absorption. Clearly, the presence of the methyl group has very little effect, as expected, on the infrared spectrum in this spectral region as both experimental spectra are quite similar. The bonding of Li^+ to both thymine and uracil, as well as the water molecule to the ion, is likely very similar for both bases.

The predicted infrared spectra for the lowest energy structures of Ura-Li^+H_2O and Thy-Li^+H_2O are presented and compared to the experimental IRMPD spectra in Figure 2 (red traces). For both species, the experimental and predicted band positions agree quite well except for the clear absence of the band associated with the asymmetric O−H stretch of the bound water molecule (see also Table 1). Previous authors of IRMPD studies[48−52] have reported that when water is ligated to an ion, the intensity of the asymmetric O−H stretch is markedly not as intense as is predicted by theoretical studies. In this case, the asymmetric stretch is expected to be much stronger than the symmetric stretch of the ligated water, yet it is unobserved.

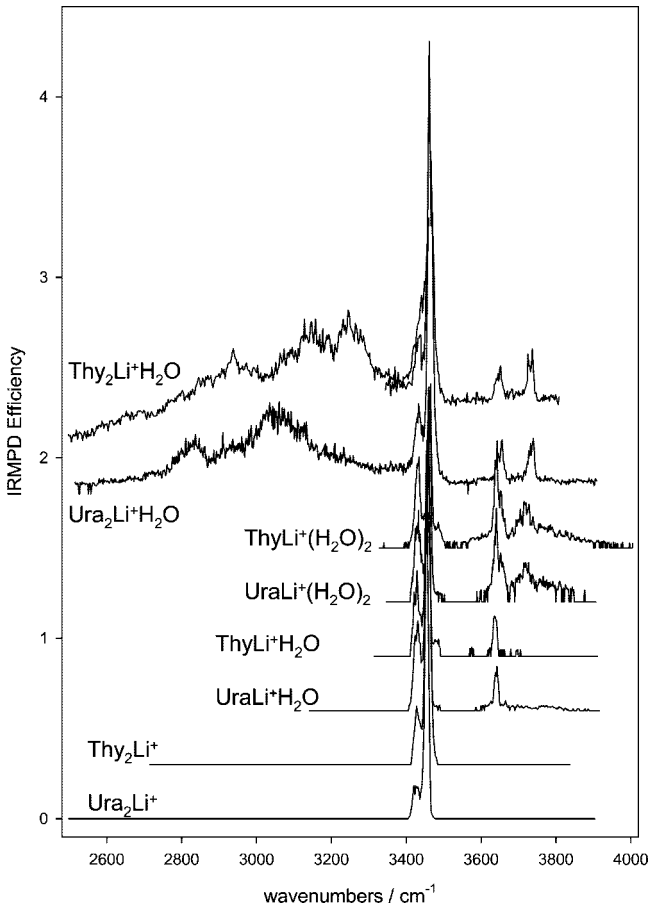

Figure 1. Comparison of all IRMPD spectra in this study. Note the similarity of the free N−H stretch region and in the positions of the water O−H stretch region for hydrated ions.

Since the photon energies resonant with the asymmetric and symmetric stretches are very similar, it is not likely that the difference in photon energy has a strong impact on the intensities of the observed features. This phenomenon has been explained recently.[50] A very important part of IRMPD spectroscopy is intramolecular vibrational energy redistribution (IVR) which immediately follows each individual photon absorption. Without strong IVR, and due to anharmonicity, subsequent photons cannot be absorbed by the ion. IVR is further dependent upon strong coupling mechanisms between the absorbing mode and other modes within the molecule. In the context of proton-bound dimers such as $NH_4^+H_2O$, Pankewitz et al.[50] explained that motion of the atoms in the symmetric O−H stretch of the ligated water is such that the oxygen atom moves along the axis of the O-ion bond and should have strong coupling with other vibrational modes. On the contrary, for the asymmetric O−H stretch, the oxygen atom moves perpendicular to the O-ion bond and would be expected to have weaker coupling to other vibrational modes. They also reported that cubic coupling constants from anharmonic calculations on $NH_4^+H_2O$ are at least 2 orders of magnitude larger for the symmetric O−H stretch than for the asymmetric O−H stretch. Results of anharmonic calculations on Ura-Li^+H_2O also reveal that the top four cubic coupling constants for the symmetric O−H stretch are approximately 2 orders of magnitude stronger than the top three coupling constants for the asymmetric stretch. The observation of the asymmetric stretch will be addressed again with respect to Ura-$Li^+(H_2O)_2$ and Ura_2-Li^+H_2O (as well as the thymine analogues).

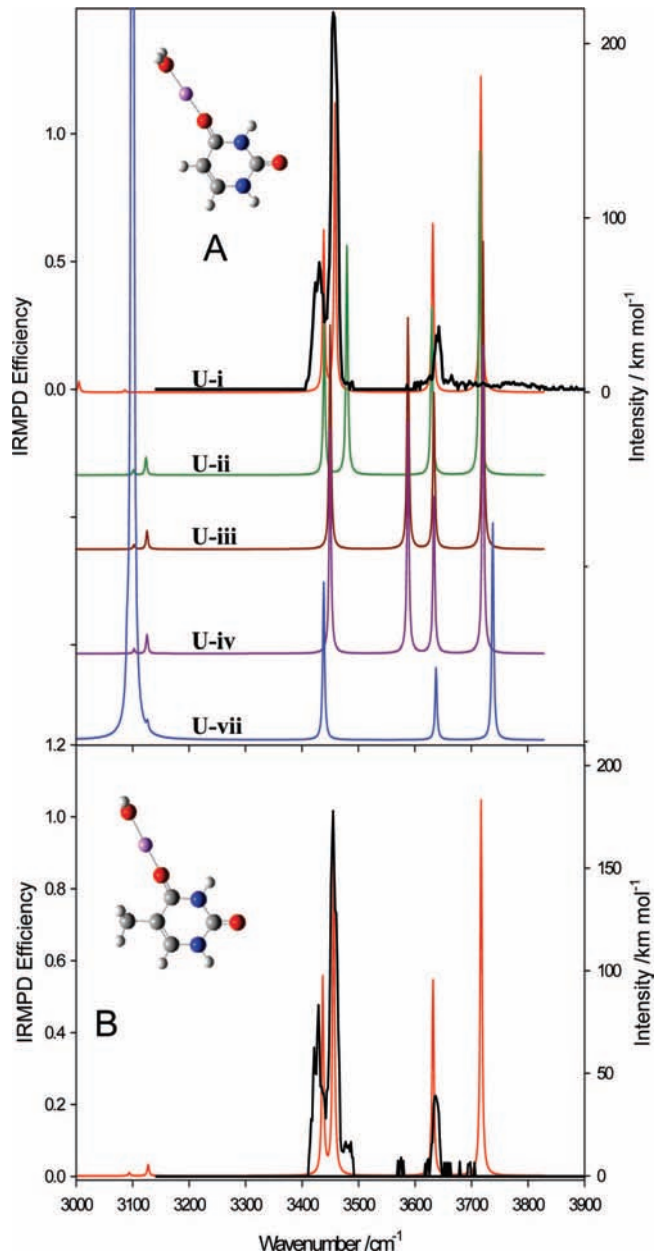

Figure 2. IRMPD spectra of (A) Ura-$Li^+(H_2O)$ and (B) Thy-$Li^+(H_2O)$ complexes overlaid with theoretical spectra of the lowest energy structures (red) as predicted by theoretical methods. In (A) some of the higher energy structures are also compared to the experimental spectra.

The IRMPD spectrum of Ura-Li^+H_2O is also compared to theoretical spectra of the four lowest energy structures (**U-i** to **U-iv**) and one higher energy structure (**U-vii**) in Figure 2A. All calculated structures for the uracil- and thymine-containing species are shown in Figure 3. An "*" indicates the position of the methyl groups in the thymine-containing species. The relative free energies are provided in Figure 3. The relative enthalpies and free energies are provided in Table S1 in the Supporting Information. As is presented here in Figure 3, and supported by previous work,[10,17] the bases were found to have two main binding sites for lithium cations, O4 and O2. The lithium cation is also the most favorable site for solvation, i.e., binding of water. It is clear from Figure 2 that the predicted spectra for both **U-i** and **U-ii** agree well with the experimentally determined IRMPD spectrum. Therefore, it is impossible to assign a structure based solely on a comparison of theoretical

TABLE 1: Experimental IRMPD Band Positions (cm^{-1}) and Assignments for B−Li^+−$(H_2O)_n$ (n = 1−2) and B_2−Li^+−$(H_2O)_m$ (m = 0−1) for B = Thymine, Uracil[a]

	mode				
complex	νOH_{asym}[d]	νOH_{sym}	νN1H	νN3H	H-bonded N−H stretch
thymine[b]			3480	3437	
Thy-Li^+H_2O	−	3635	3455	3429	
(**T-i**)	(3718)	(3632)	(3459)	(3439)	
Thy-$Li^+(H_2O)_2$	3720	3643	3463	3433	
(**T-I**)	(3737)	(3645)	(3464)	(3441)	
Thy_2-Li^+			3460	3427	
(**T-a**)			(3463)	(3441)	
Thy_2-Li^+H_2O	3730	3652	3459	3439	3250, 3150, 2937
uracil[c]			3484	3435	
			3479		
			3473		
Ura-Li^+H_2O	−	3643	3455	3431	
(**U-I**)	(3718)	(3632)	(3456)	(3437)	
Ura-$Li^+(H_2O)_2$	3718	3641	3459	3430	
(**U-I**)	(3737)	(3645)	(3460)	(3438)	
Ura_2-Li^+			3456	3428	
(**U-a**)			(3460)	(3439)	
Ura_2-Li^+H_2O	3739	3656	3462	3435	3060, 2850

[a] Scaled theoretical values are also reported in parentheses. B3LYP/6-31+G(d,p) scaled by 0.958. [b] From matrix isolation spectrum of thymine in argon.[41,42] [c] From matrix isolation spectrum of uracil in argon.[39] [d] Values noted with a "−" are unobserved as discussed in text.

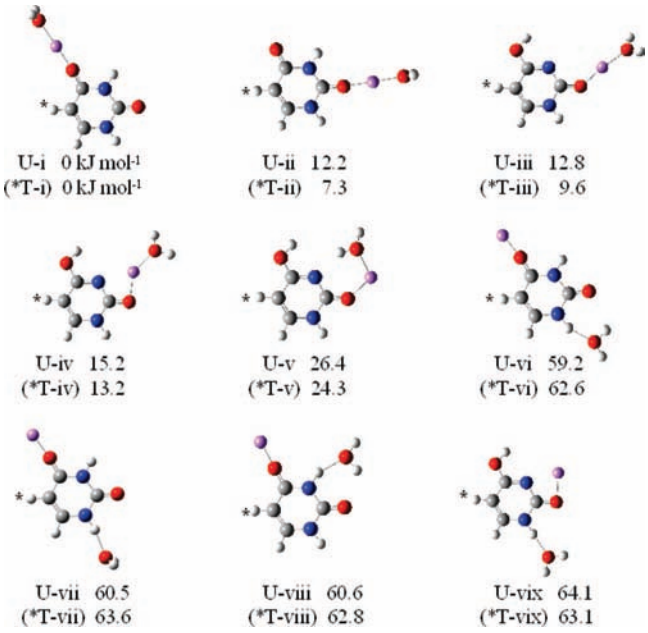

Figure 3. Structures of B−$Li^+(H_2O)$ complexes as determined by theoretical methods as well as MP2/6-311++G(2d,p)//B3LYP/6-31+G(d,p) relative free energies. Relative enthalpies can also be seen in Table S1. The asterisk indicates the position of the methyl group in the thymine-containing species.

and experimental spectra in this range. However, in structures **U-i** and **T-i**, binding of the $(H_2O)Li^+$− to the O4 site was found to be more favorable by 12.2 and 7.3 kJ/mol for uracil and thymine, respectively, over the O2 site. These results are similar to those obtained by Rodgers and Armentrout[10] and Del Bene[17] on uracil and thymine which showed the O4 site to be preferred by lithium cation over the O2 site by a stabilization energy of approximately 14 and 6 kJ mol^{-1}, respectively. Based on this difference, one can say that the O4 structure is, if not the sole binding site, more heavily populated in the gas phase. The experimental spectra for both Ura-Li^+H_2O and Thy-Li^+H_2O are certainly consistent with **U-i** and **T-i** being the structure.

Theoretical studies have shown that the **T2** tautomer (Scheme 1) is lowered in energy beyond that of the canonical (**T1**) form when bound to other metals (e.g., Na^+, Mg^{2+}).[8] The energy difference between the free tautomers of thymine **T1/T2** and uracil **U1/U2** in the gas phase before metalation by a lithium ion has been reported to be 49.6 and 53.7 kJ mol^{-1}, respectivey,[15] in favor of the canonical form. Based on this large difference in energy, it has been assumed that the canonical form would be the solely existing form in the gas phase and thus be more susceptible to bonding with a lithium cation.[15] This is further supported by microwave spectral work that has shown the diketo structure (**T1**) of thymine to be the most stable tautomeric form in the gas phase over the enol (**T2**).[53] In this study, the lithiated thymine and uracil cations are formed in aqueous solution, so a possibility exists that the **U2** and **T2** tautomers are formed in the presence of lithium cation. However, the **U2** tautomers **U-iii** and **U-iv** can be ruled out by comparing the experimental and predicted spectra as seen in Figure 2A. The absence of a second band in the 3450 cm^{-1} region in the theoretical spectrum is not necessarily an indicator of the absence of this structure from the mixture. However, an O−H stretching vibration from the enol tautomer is predicted to occur about 3590 cm^{-1}, but this feature is absent in the IRMPD spectrum. Furthermore, these structures are determined to be higher in free energy than the canonical form by ∼13−15 $kJmol^{-1}$. **U-v** can also be ruled out based upon the absence of a strongly red-shifted O−H stretch of water in the experimental spectrum and based on its predicted thermochemistry. The **T1/U1** diketo structures are thus concluded to be the major contributors, and of most importance in this work.

It is unfortunate that the spectra were not also recorded in the slightly lower energy spectra region since it would have been possible to spectroscopically determine the presence of structures such as **U-vii**, **U-viii**, and **U-ix**, where water is not bound to the lithium ion. The hydrogen-bonded−N−H stretch is expected to occur at around 3100 cm^{-1}. However, these structures are predicted to be significantly higher in energy and therefore probably not important isomers in this work.

3.2. Ura-$Li^+(H_2O)_2$ and Thy-$Li^+(H_2O)_2$. The lowest energy structures predicted for Ura-$Li^+(H_2O)_2$ and Thy-$Li^+(H_2O)_2$ complexes involve binding of both water molecules to the lithium ion of the Ura-Li^+ and Thy-Li^+ cores. The predicted spectra for **U-I** and **T-I** are compared to the experimental IRMPD results in Figure 4, and it is clear that there is very good agreement between the theoretical and experimental spectra (see Figure 5 for structures). In Table 1, it is also seen that the N−H and O−H stretching vibrations are in similar positions for the monohydrated and doubly hydrated species. The positions of the experimental NH stretching vibrations at N3 and N1 positions are ∼3430 and ∼3460 cm^{-1}, respectivey, and are unchanged for both the monohydrated and dihydrated species. This suggests that the bonding of H to N is similar in all structures, or in other words, the addition of lithium, water, or second base affects the NH group in a like manner in each structure.

It can be seen in the present case that the O−H asymmetric stretching vibrations are observed; however, the ratio of the intensities of the asymmetric stretch to the symmetric stretch (I_{ν_3}/I_{ν_1}) is still less than those predicted. If one compares the ratio of the peak areas, ν_3 and ν_1 are of comparable intensity, not the expected 2:1 intensity predicted by theory. Pankewitz et al.[50] noticed that the smaller the binding energy of water to

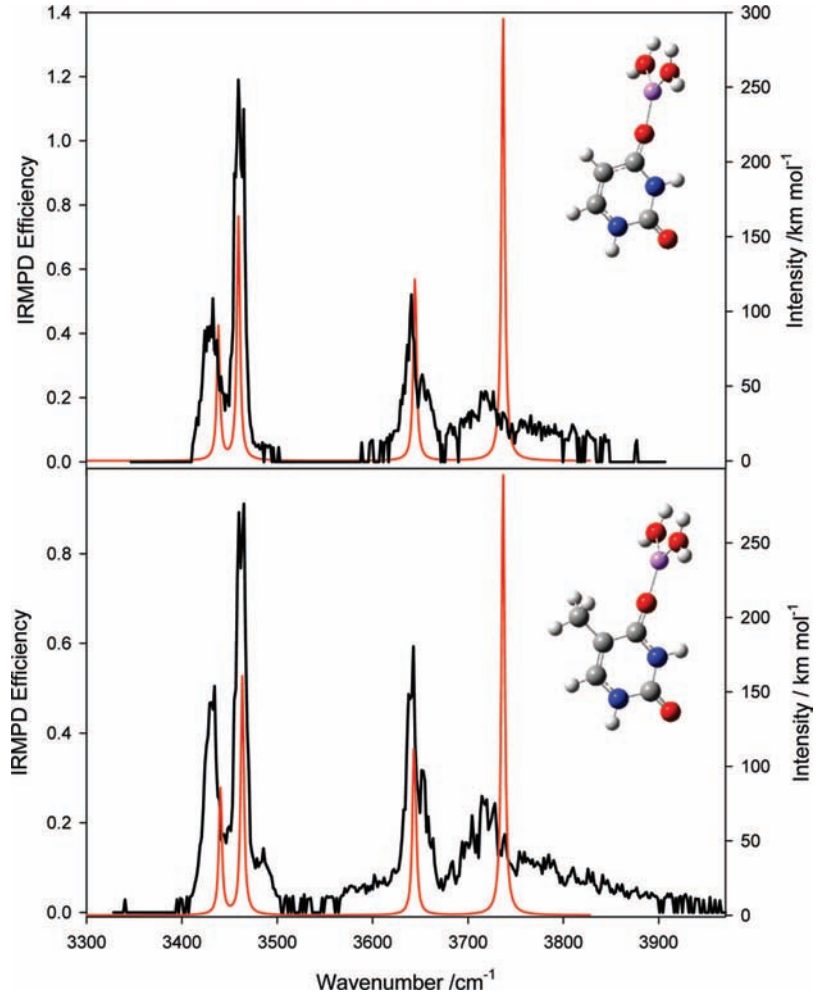

Figure 4. IRMPD spectra of Ura-$Li^+(H_2O)_2$ and Thy-$Li^+(H_2O)_2$ overlaid with theoretical spectra (red) of the lowest energy structures as predicted by theoretical methods. In each case, experimental and theoretical spectra for the lowest energy isomers are in very good agreement.

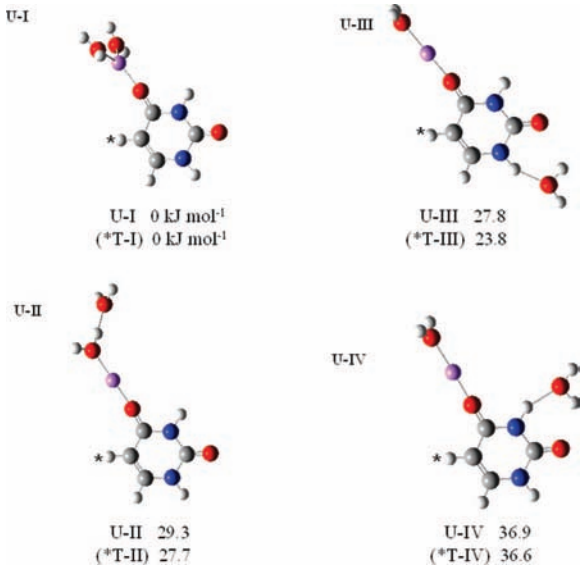

Figure 5. Structures of B−$Li^+(H_2O)_2$ complexes as determined by theoretical methods as well as MP2/6-311++G(2d,p)//B3LYP/6-31+G(d,p) relative free energies. Relative enthalpies can also be seen in Table S2. The asterisk indicates the position of the methyl group in the thymine-containing species.

the central ion, the larger the observed I_{ν_3}/I_{ν_1}. The MP2/6-311++G(2d,p)//B3LYP/6-31+G(d,p) 298 K dissociation energies are 78 and 114 kJ mol^{-1} to remove the second and first water molecule, respectively, for both the uracil and thymine systems, which is consistent with the observations of Pankewitz et al.[50] This observation could indicate that fewer photons are necessary to observe dissociation or that coupling is stronger for a more loosely bound system. Anharmonic calculations for Ura-$Li^+(H_2O)_2$ predict the cubic coupling constants for the symmetric stretch to be larger than the asymmetric stretch, but in this case the difference is less than 1 order of magnitude.

The experimental IRMPD spectra are consistent with the predicted infrared spectra for the lowest energy structures of both Ura-$Li^+(H_2O)_2$ and Thy-$Li^+(H_2O)_2$. The higher energy structures can be seen in Figure 5 along with their relative free energies. The relative enthalpies and free energies are also provided in Table S2 in the Supporting Information. Spectroscopically, it is difficult to completely rule them out. In all three higher energy structures, there is expected to be a band below 3300 cm^{-1} which is outside our observed spectral range for these species. The hydrogen-bonded O−H stretch for **U-II** and **T-II** are expected to occur around 3220 cm^{-1} while the hydrogen-bonded N−H stretches are expected to occur at about 3180 cm^{-1}. As well, for all three species the region between the asymmetric stretching vibration and the N−H stretching region is predicted to be more complicated due to the nonsymmetric nature of the structures. The breadth of the observed bands may mask these other bands, but in our opinion, the experimental spectra and the large difference in energies between the lowest

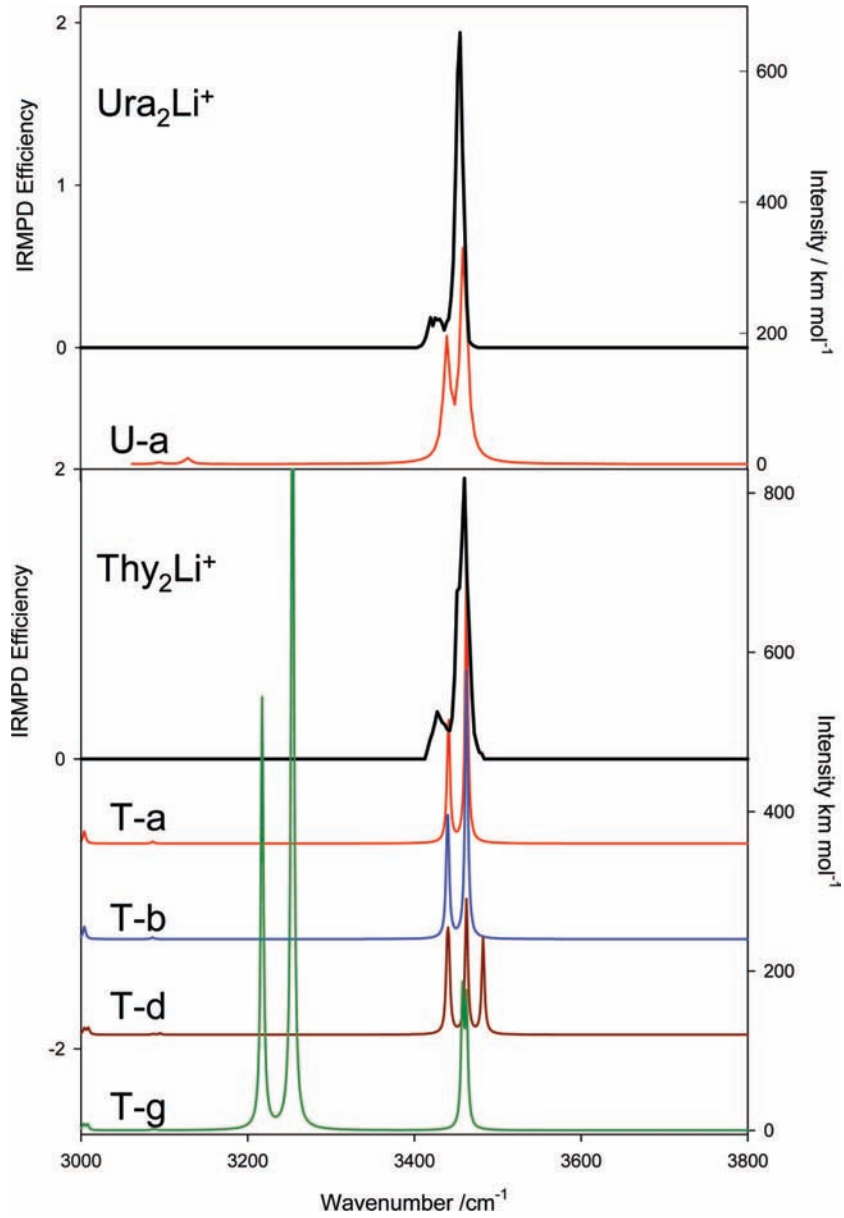

Figure 6. IRMPD spectra of Ura_2-Li^+ and Thy_2-Li^+ overlaid with theoretical spectra (red) of the lowest energy structures as predicted by theoretical methods. Additional predicted spectra of higher energy isomers (**T-b**, **T-d**, **T-g**) are also shown for comparison.

and higher energy isomers suggest that the most likely structures of the observed ions are those of **U-I** and **T-I**.

3.3. Ura_2-Li^+ and Thy_2-Li^+. The experimental spectra of the lithium-bound dimer of uracil and thymine are very similar to one another as is seen in Figure 6. As well, they are quite simple spectra comprised of two resolved features which are assigned to the N−H stretching vibrations (Table 1). Experimental spectra for Ura_2-Li^+ and Thy_2-Li^+ are also compared with computed spectra for the lowest energy structures (for structures see Figure 7), and, for the latter, predicted spectra for a number of the higher energy structures are also presented. Dimers where the lithium cation is bound to O4 of each moiety are lowest in energy (Figure 7 and Table S3), with the most favorable structure being a planar orientation. For Ura_2Li^+, there are three structures which are very similar in energy (**U-a**, **U-b**, and **U-c**). For Thy_2Li^+, the corresponding **T-c** structure does not exist as a consequence of steric constraints due to the methyl groups. While the predicted spectrum for the lowest energy structure matches the IRMPD spectra obtained, these other structures (such as **T-b**) can certainly not be ruled out by comparing the predicted and experimental spectra, nor by thermochemical arguments, and they probably coexist.

Structures **T-d** and **T-e** are similar to each other (as are **U-d** and **U-e**) except for rotation about the O−Li^+−O axis. These two structures have Li^+ bound to O4 of one base and O2 of the other such that symmetry of the lithium ion-bound dimer is broken, resulting in three predicted bands in the N−H stretch region. The experimental spectra clearly do not provide any evidence for a third band, and it can be concluded that these isomers do not exist in the present experiments. The predicted thermochemistry in this case is not as conclusive but is still consistent with this conclusion. Structure **T-g** and **U-g** have similar spectra to the lowest energy structures and cannot be ruled out by spectroscopic arguments, but since they are considerably more thermodynamically unstable compared to **T-e** and **T-d** (and the uracil analogues), they are not likely present in a significant abundance. Another set of higher energy structures, **T-f** and **U-f**, are considered based on the results of the hydrated lithium ion-bound dimer discussed in the next section. These structures, bent about Li^+, are stabilized due to

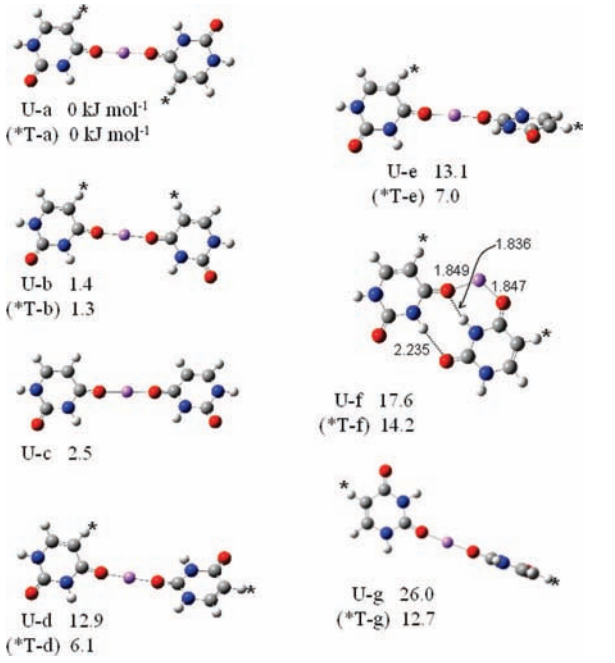

Figure 7. Structures of B_2−Li^+ complexes as determined by theoretical methods as well as MP2/6-311++G(2d,p)//B3LYP/6-31+G(d,p) relative free energies. Relative enthalpies can also be seen in Table S3. The asterisk indicates the position of the methyl group in the thymine-containing species.

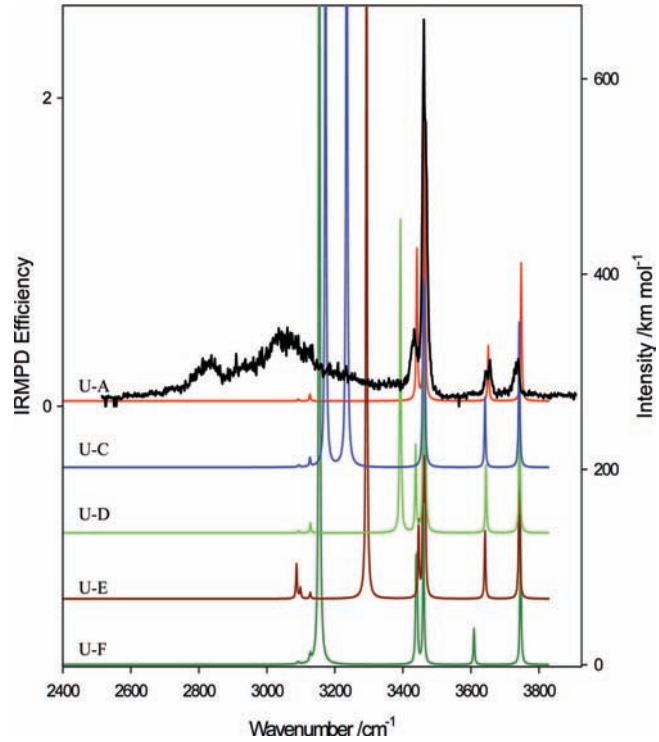

Figure 8. IRMPD spectrum of Ura_2-Li^+H_2O overlaid with theoretical spectra of the lowest energy structures as predicted by theoretical methods. Corresponding structures can be seen in Figure 9.

the hydrogen bonding so that they are actually similar in enthalpy to **T-a** and **U-a** (Table S3). Also, due to the hydrogen bonding, they are fairly tight structures so that they are much less favorable from an entropic viewpoint. The predicted spectrum for **T-f** has two hydrogen-bonded N−H stretching vibrations red-shifted to between 3200 and 3300 cm^{-1}. Clearly (Figure 7), the experimental spectrum shows no evidence for **T-f**.

3.4. Ura_2-Li^+H_2O and Thy_2-Li^+H_2O. The addition of water to both Ura_2-Li^+ and Thy_2-Li^+, as demonstrated in Figure 1, results in a far richer IRMPD spectrum. In both systems, the two bands assigned to the N−H stretching vibrations are virtually unchanged by the addition of water. There are also two sharp bands assigned to the water asymmetric O−H stretch and symmetric O−H stretching vibrations, which are both clearly visible. The I_{ν_3}/I_{ν_1} are between 1 and 1.5 for both systems, and the MP2/6-311++G(2d,p)//B3LYP/6-31+G(d,p) binding energies of water to these complexes are between 65 and 70 kJ mol^{-1}. The I_{ν_3}/I_{ν_1} are still slightly lower than expected by calculations (see Figures 8 and S2).

Interestingly, there are broad bands in the 2500−3400 cm^{-1} region which must obviously be due to the influence of water. The position and shape of these features are typical of hydrogen-bonded N−H or O−H stretching vibrations. There are two possibilities for the modes responsible for these absorptions. Since both the asymmetric and symmetric stretching vibrations of water are accounted for, presumably water is not acting as a hydrogen bond donor. Therefore it is the N−H bonds which are acting as hydrogen-bonding donors and are responsible for the bands between 2500 and 3400 cm^{-1}. The other option is that these features are due to hydrogen-bonded O−H stretches where water is the hydrogen-bonding donor and there is more than one structure responsible for the observed IRMPD spectra. Of course these two options do not exclude one another. It would not be expected that structures corresponding with the **U2** or **T2** isomers are formed since in section 3.3 it is was concluded that these isomers do not exist under the present experimental conditions.

For both Ura_2-Li^+H_2O and Thy_2-Li^+H_2O, five structures were found to be relatively similar in free energy (Figure 9 and Table S4). IRMPD spectra with overlaid theoretical spectra for Ura_2-Li^+H_2O and Thy_2-Li^+H_2O are shown in Figures 8 and S2, respectively. It is fairly clear that none of the single theoretical spectra account for the experimental spectra completely, and since all five structures lie within just a few kJ mol^{-1} in free energy, they may all be contributors to the experimental IRMPD spectrum. Structures **U-A** and **U-B** as well as **T-A** and **T-B** have trigonal planar geometries of the two bases and water about the central lithium ion. These structures clearly cannot account for the broad features between 2500 and 3400 cm^{-1}, but this does not rule them out as contributing to the overall IRMPD spectrum.

The structures with the lowest relative enthalpy are **U-C** and **T-C**, respectively, for the uracil and thymine systems and are of particular interest. Taking entropy into account, the **T-C** and **U-C** isomers are only slightly higher in free energy over **T-D** and **U-A**, respectively (Figure 9 and Table S4). These structures contain two intramolecular hydrogen bonds between carbonyl oxygen atoms of one base and the N−H of the second base. This type of interbase hydrogen bonding is a feature of base pairing in the Watson−Crick model. Hydrogen bonding is characterized in the infrared spectrum by a shift of the N−H stretching vibration to lower frequency.[54] As is seen in Figures 8 and S2 for the solvated dimer of uracil and thymine, the shift of NH stretching frequencies to about 3200 cm^{-1} corresponds to bands in the experimental spectrum. For Ura_2-Li^+H_2O, the experimental bands are considerably more red-shifted than predicted. These strong hydrogen bonds are quite anharmonic in nature so the harmonic calculations are not expected to quantitatively account for their band positions as they would

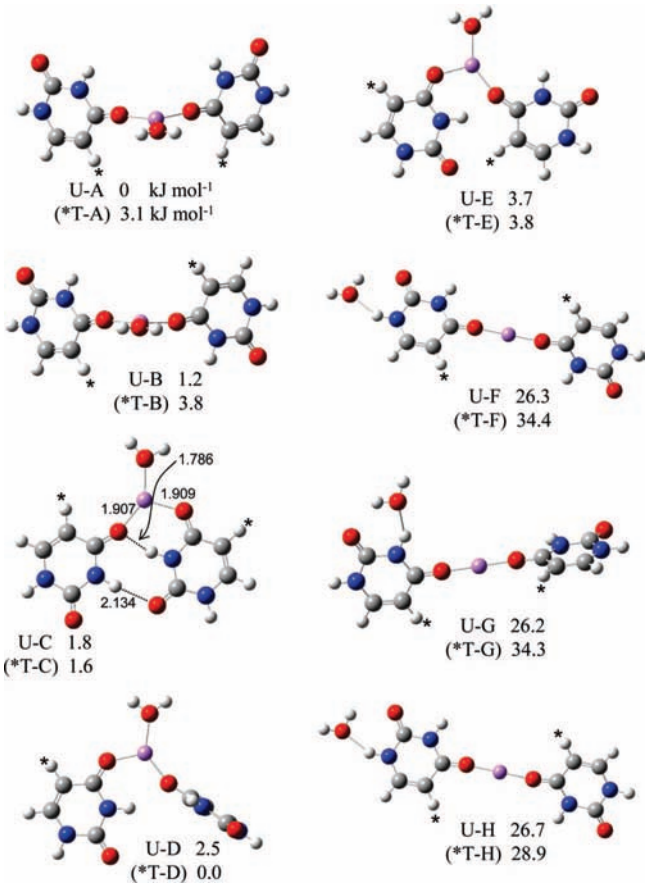

Figure 9. Structures of Ura_2-Li^+H_2O as determined by theoretical methods as well as MP2/6-311++G(2d,p)//B3LYP/6-31+G(d,p) relative free energies. Relative enthalpies can also be seen in Table S1. The asterisk indicates the position of the methyl group in the thymine-containing species.

for less anharmonic modes. Careful comparison of the calculated and experimental spectra reveals that **U-C** and **T-C** do not alone account for the experimental spectra. Due to hydrogen bonding, there is only one feature corresponding to the non-hydrogen-bonded N−H stretch.

Structures **U-D** and **U-E**, as well as **T-D** and **T-E**, have only one hydrogen-bonded N−H moiety and are therefore higher in enthalpy than **U-C** and **T-C**. However, due to the increased entropic stability, they are similar in free energy to **U-C** and **T-C**. While the experimental bands are, again, at significantly lower energy than the predicted bands, it is impossible to rule these structures out based on the IRMPD spectra. As discussed above, these anharmonic bands are not necessarily quantitatively reproduced by the harmonic calculations. The experimental IRMPD spectrum for Ura_2-Li^+H_2O has at least two resolved bands, while that for Thy_2-Li^+H_2O has three bands below 3400 cm^{-1}. This could mean that there are less structural isomers contributing to the spectrum, but this is only speculation.

Structures **U-F**, **U-G**, and **U-H** for Ura_2-Li^+H_2O as well as structures **T-F**, **T-G** and **T-H** for Thy_2-Li^+H_2O are very similar as are their predicted spectra. Water is not bound to Li^+, but to the DNA base. Only the predicted spectrum for **U-F** is compared with the IRMPD spectrum of Ura_2-Li^+H_2O in Figure 8. The symmetric O−H stretch doesn't exist for these structures since water is now asymmetric, containing one weakly hydrogen-bonded O−H and one free O−H. The bands assigned to the symmetric stretch of water at 3656 cm^{-1} for Ura_2-Li^+H_2O and 3652 cm^{-1} for Thy_2-Li^+H_2O are in a similar position if not slightly blue-shifted compared to the symmetric stretch assigned for Ura-Li^+H_2O, Thy-Li^+H_2O, Ura-$Li^+(H_2O)_2$, and Thy-$Li^+(H_2O)_2$ above. For the structures where water is bound to the DNA base, the hydrogen-bonded O−H stretch is predicted to occur at a significantly lower wavenumber value, 3607 cm^{-1}. Structures **U-F**, **U-G**, and **U-H** and **T-F**, **T-G**, and **T-H** are higher in free energy than the lowest energy structures by some 25−35 kJ mol^{-1} which allows them to be ruled out based on energetic grounds.

Bush et al.[55] observed large structural effects upon the addition of one water molecule to lithiated arginine cation. While the nonzwitterionic form of lithiated arginine cation is the lowest energy form, addition of one water molecule stabilizes the zwitterions by some 25−32 kJ mol^{-1}. This zwitterion structure is further stabilized by an intramolecular hydrogen bond between the carboxyl group and the protonated side chain.

It is worthwhile to examine more closely the effect of the water molecule on the structure of the lithium-bound uracil and thymine homodimers. Structures **U-f** and **T-f** in Figure 7 are low in relative enthalpy, **T-f** being the global minimum as far as enthalpy is concerned (Table S3). These structures owe their stabilities to the two intermolecular hydrogen bonds. However, due to the tightness of these structures, they are entropically disfavored resulting in a significantly higher free energy relative to other structures (Table S3). **U-f** and **T-f** resemble structures **U-C** and **T-C** in Figure 9 except the former do not have a water molecule attached. **U-C** and **T-C** are by far the most favored structures in terms of enthalpy. The enthalpic stability and low entropy of these structures result in free energies which are among the lowest and make these structures energetically favorable (Table S3). For clarity, only the uracil complexes will be considered in the rest of this discussion. Inspection of both **U-f** and **U-c** (latter solvated with water, Figures 7 and 9, respectively) reveals very similar structures as stated above. Both have two intermolecular hydrogen bonds and are low-entropy structures. The presence of a strong water−Li^+ interaction relaxes to some extent the two uracil−Li^+ interactions. The uracil−Li^+ bond distances both stretch from 1.85 to 1.91 Å upon the addition of water. This allows for greater hydrogen-bonding interactions as the two uracil molecules can get closer together. The hydrogen bonds in **U-f** are 2.235 and 1.836 Å, whereas in the hydrated complex they are substantially shorter, 2.134 and 1.786 Å, and therefore significantly stronger. The shorter intramolecular hydrogen bonds in **U-C** are responsible for the increased stability of this strongly hydrogen-bonded structure.

4. Summary

Metalation of thymine and uracil by lithium cation was investigated by IRMPD spectroscopy in conjunction with a theoretical study at the B3LYP/6-31+G(d,p) and MP2/6-311++G(2d,p)//B3LYP/6-31+G(d,p) levels of theory and basis sets. Solvation of the complexes by the first two water molecules was investigated for the monomers and by one molecule for the lithium-bound dimer. The predicted structures are reported for each case. A comparison of experimental and theoretical spectra was performed to determine the most probable structures for each case. Thermochemical information for each structure is also reported and was used in suggesting probable structures as major contributors in the gas phase. With no single structure being able to attribute for all peaks observed in the IRMPD spectra of Ura_2-Li^+H_2O and Thy_2-Li^+H_2O, a mixture of a number of low-energy structures is proposed as contributing to experimental results.

In all cases, the lithium ion was found to bond most favorably with the O4 oxygen of the base, with water molecules binding

to the lithium ion. Experimental spectra obtained for Ura-Li^+H_2O, Thy-Li^+H_2O, Ura-$Li^+(H_2O)_2$, Thy-$Li^+(H_2O)_2$, Ura_2-Li^+, and Thy_2-Li^+ are similar to one another in the N−H stretching region, suggesting similar structures in each case. This was supported through theoretical results. Richer spectra for Ura_2-Li^+H_2O and Thy_2-Li^+H_2O indicate the presence of inter-base intramolecular hydrogen bonding between the DNA bases as well as a number of other low-energy structures that are predicted to be thermodynamically stable in the gas phase and whose predicted infrared spectra are consistent with the experimental IRMPD spectra.

It is also worthwhile mentioning in the conclusions that hydrated species contain the spectral peculiarity inherent in consequence spectroscopy, the much smaller than expected I_{ν_3}/I_{ν_1}. Other than $NO^+(H_2O)$,[49] Ura-Li^+H_2O and Thy-Li^+H_2O, are the only other species for which an intense asymmetric O−H stretch of the water moiety is expected but is nonexistent. Anharmonic calculations on these species are consistent with the explanation first proposed by Pankewitz et al.[50] that poor coupling of this mode to other modes within the ion acts as an IVR bottleneck preventing further photon absorption and therefore dissociation.

Acknowledgment. We are grateful for the generous financial support of our work by the Natural Sciences and Engineering Research Council of Canada (NSERC). The computational resources of both the Atlantic Computational Excellence Network (ACE-Net) and the Western Canada Research Grid (WestGrid) are gratefully acknowledged. E.A.L.G. acknowledges the CGS-M granted by NSERC. The financial support of the European Commission through EPITOPES is also acknowledged as is the technical assistance of T. Besson.

Supporting Information Available: Complete ref 45 and tables of relative enthalpies and free energies for isomeric structures as well as the spectrum for $Thy_2Li^+H_2O$. This material is available free of charge via the Internet at http://pubs.acs.org/.

References and Notes

(1) Saenger, W. *Principles of Nucleic Acid Structure*; Springer-Verlag: New York, 1984; pp 201−210.
(2) Cerda, B. A.; Wesdemiotis, C. *J. Am. Chem. Soc.* **1996**, *118*, 11884.
(3) *Metal Ions in Biological Systems: Studies of Some biochemical and Environmental Problems*; Dhar, S. K., Ed.; Plenum: New York, 1973; Vol. 40, pp 43−66.
(4) McFail-lsom, L.; Sines, C. C.; Williams, L. D. *Curr. Opin. Struct. Bio.* **1999**, *9*, 298.
(5) Shui, X.; Sines, C. C.; McFail-Isom, L.; VanDerveer, D.; Williams, L. D. *Biochemistry* **1998**, *37*, 16877.
(6) *Nucleic Acids in Chemistry and Biology*; Blackburn, G. M., Gait, M. J., Eds.; Oxford University Press: Oxford, 1990; pp 19−26.
(7) Guillaumont, S.; Tortajada, J.; Salpin, J.-Y.; Lamsabhi, A. M. *Int. J. Mass Spectrom.* **2005**, *243*, 279.
(8) Kabelac, M.; Hobza, P. *J. Phys. Chem. B* **2006**, *110*, 14515.
(9) Koch, K. J.; Aggerholm, T.; Nanita, S. C.; Cooks, R. G. *J. Mass Spectrom.* **2002**, *37*, 676.
(10) Rodgers, M. T.; Armentrout, P. B. *J. Am. Chem. Soc.* **2000**, *122*, 8548.
(11) Russo, N.; Toscano, M.; Grand, A. *J. Am. Chem. Soc.* **2001**, *123*, 10272.
(12) Rochut, S.; Pepe, C.; Paumard, J. P.; Tabet, J. C. *Rapid Commun. Mass Spectrom.* **2004**, *18*, 1686.
(13) Yang, Z.; Rodgers, M. T. *J. Am. Chem. Soc.* **2004**, *126*, 16217.
(14) Zhu, W.; Luo, X.; Puah, C. M.; Tan, X.; Shen, J.; Gu, J.; Chen, K.; Jiang, H. *J. Phys. Chem. A* **2004**, *108*, 4008.
(15) Russo, N.; Toscano, M.; Grand, A. *J. Phys. Chem. B* **2001**, *105*, 4735.
(16) Monajjemi, M.; Ghiasi, R.; Passdar, H.; Mollaamin, F.; Ketabi, S.; Asaddian, F.; Chahkandi, B.; Karimkhani, M. *J. Mol. Design* **2003**, *2*, 741.
(17) del Bene, J. E. *J. Phys. Chem.* **1984**, *88*, 5927.
(18) Rodgers, M. T.; Armentrout, P. B. *Int. J. Mass Spectrom.* **2007**, *267*, 167.
(19) Gould, I. R.; Burton, N. A.; Hall, R. I.; Hillier, I. H. *J. Mol. Struct. (Theochem)* **1995**, *33*, 147.
(20) Estrin, D. A.; Paglieri, L.; Corongiu, G. *J. Phys. Chem.* **1994**, *98*, 5653.
(21) Buda, A.; Sygula, A. *THEOCHEM* **1983**, *9*, 255.
(22) Salpin, J.-Y.; Guillaumont, S.; Tortajada, J.; MacAleese, L.; Lemaire, J.; Maitre, P. *Chem. Phys. Chem.* **2007**, *8*, 2235.
(23) Casaes, R. N.; Paul, J. B.; McLaughlin, R. P.; Saykally, R. J.; van Mourik, T. *J. Phys. Chem. A* **2004**, *108*, 10989.
(24) Del Bene, J. E. *J. Chem. Phys.* **1982**, *76*, 1058.
(25) Dolgounitcheva, O.; Zakrzewski, V. G.; Ortiz, J. V. *J. Phys. Chem. A* **1999**, *103*, 7912.
(26) Gadre, S. R.; Babu, K.; Rendell, A. P. *J. Phys. Chem. A* **2000**, *104*, 8976.
(27) Gaigeot, M. P.; Kadri, C.; Ghomi, M. *J. Mol. Struct.* **2001**, *565*−*566*, 469.
(28) Ilich, P.; Hemann, C. F.; Hille, R. *J. Phys. Chem. B* **1997**, *101*, 10923.
(29) Kim, N. J.; Kim, Y. S.; Jeong, G.; Ahn, T. K.; Kim, S. K. *Int. J. Mass Spectrom.* **2002**, *219*, 11.
(30) Kim, S.; Wheeler, S. E.; Schaefer, H. F. *J. Chem. Phys.* **2006**, *124*, 204310.
(31) Ohta, Y.; Tanaka, H.; Baba, Y.; Kagemoto, A.; Nishimoto, K. *J. Phys. Chem.* **1986**, *90*, 4438.
(32) van Mourik, T. *Phys. Chem. Chem. Phys.* **2001**, *3*, 2886.
(33) van Mourik, T.; Benoit, D. M.; Price, S. L.; Clary, D. C. *Phys. Chem. Chem. Phys.* **2000**, *2*, 1281.
(34) van Mourik, T.; Price, S.; Clary, D. *Faraday Discuss.* **2001**, *118*, 95.
(35) van Mourik, T.; Price, S. L.; Clary, D. C. *J. Phys. Chem. A* **1999**, *103*, 1611.
(36) Kryachko, E. S.; Nguyen, M. T.; Zeegers-Huyskens, T. *J. Phys. Chem. A* **2001**, *105*, 1934.
(37) Colarusso, P.; Zhang, K.; Guo, B.; Bernath, P. F. *Chem. Phys. Lett.* **1997**, *269*, 39.
(38) Gould, I. R.; Vincent, M. A.; Hillier, I. H. *J. Chem. Soc., Perkin Trans. 2* **1992**, 69.
(39) Ivanov, A. Y.; Plokhotnichenko, A. M.; Radchenko, E. D.; Sheina, G. G.; Blagoi, Y. P. *J. Mol. Struct.* **1995**, *372*, 91.
(40) Szczepaniak, K.; Szczesniak, M. M.; Person, W. B. *J. Phys. Chem. A* **2000**, *104*, 3852.
(41) Graindoyrze, M.; Smets, J.; Zeegers-huyskens, T.; Maes, G. *J. Mol. Struct.* **1990**, *222*, 345.
(42) Lés, A.; Adamowicz, L.; Nowak, M.; Lapinski, L. *Spectrochim. Acta, Part A* **1992**, *48*, 1385.
(43) Bakker, J. M.; Besson, T.; Lemaire, J.; Scuderi, D.; Maitre, P. *J. Phys. Chem. A* **2007**, *111*, 13415.
(44) Rajabi, K.; Easterling, M. L.; Fridgen, T. D. *J. Am. Soc. Mass Spectrom.*, submitted for publication.
(45) Frisch, M. J. T.; et al. *Gaussian 03*, revision C.02; Gaussian, Inc.: Wallingford CT, 2004.
(46) Dennington, R., II; Keith, T.; Millam, J.; Eppinnett, K.; Hovell, W. L.; Gilliland, R. *GaussView*, Version 3.0; Semichem, Inc.: Shawnee Mission, KS, 2003.
(47) Merrick, J. P.; Moran, D.; Radom, L. *J. Phys. Chem. A* **2007**, *111*, 11683.
(48) Bush, M. F.; Saykally, R. J.; Williams, E. R. *Chem. Phys. Chem.* **2007**, *8*, 2245.
(49) Choi, J.-H.; Kuwata, K. T.; Haas, B.-M.; Cao, Y.; Johnson, M. S.; Okumura, M. *J. Chem. Phys.* **1994**, *100*, 7153.
(50) Pankewitz, T.; Lagutschenkov, A.; Niedner-Schatteburg, G.; Xantheas, S. S.; Lee, Y.-T. *J. Chem. Phys.* **2007**, *126*, 074307.
(51) Vaden, T. D.; Lisy, J. M.; Carnegie, P. D.; Pillai, E. D.; Duncan, M. A. *Phys. Chem. Chem. Phys.* **2006**, *8*, 3078.
(52) Yeh, L. I.; Okumura, M.; Myers, J. D.; Price, J. M.; Lee, Y. T. *J. Chem. Phys.* **1989**, *91*, 7319.
(53) Brown, R. D.; Godfrey, P. D.; McNaughton, D.; Pierlot, A. P. *J. Chem. Soc., Chem. Commun.* **1989**, *1*, 37.
(54) Joesten, M. D.; Schaad, L. J. *Hydrogen Bonding*; Marcel Dekker: New York, 1974; pp 1−54.
(55) Bush, M. F.; Prell, J. S.; Saykally, R. J.; Williams, E. R. *J. Am. Chem. Soc.* **2007**, *129*, 13544.

JP809993K